HemaSphere

EHA EUROPEAN HEMATOLOGY ASSOCIATION

Letter
Open Access

IRE-dependent Regulation of Intestinal *Dmt1* Prevails During Chronic Dietary Iron Deficiency but is Dispensable in Conditions of Acute Erythropoietic Stress

Maria Qatato[1], Michael Bonadonna[1,2], Gaël Palais[1], Alina Ertl[1], Gabriele Schmidt[3], Maria Polycarpou-Schwarz[1], Zoubida Karim[4], Bruno Galy[1]

Correspondence: Bruno Galy (b.galy@dkfz.de).

Iron must be supplied in adequate amounts to sustain erythropoiesis while avoiding toxic iron accumulation.[1] Whole body iron levels are largely determined by the rate of dietary iron absorption in the duodenum.[2] Divalent metal transporter 1 (DMT1, encoded by *Slc11a2*) is an essential iron transporter present at the apical membrane of absorptive enterocytes.[3] It mediates the influx of nonheme iron from the intestinal lumen into the interior of the cell after reduction of the metal by CYBRD1 (a.k.a. DCYTB); iron is then either stored intracellularly into nanocages made of ferritin-H (FTH1) and -L (FTL1) subunits, or exported into the circulation by the basolaterally expressed transporter ferroportin (FPN, a.k.a. *SLC40A11*) to be loaded onto transferrin after oxidation of the metal by hephaestin (HEPH).[4]

Intestinal iron absorption is systemically modulated by the hormone hepcidin (a.k.a. HAMP), which binds to and inhibits its FPN.[5] Hepcidin production in hepatocytes augments when serum iron levels and body iron stores are elevated; conversely, stimulation of erythropoiesis suppresses hepcidin through the erythroblast-derived hormone erythroferrone (ERFE, encoded by *Fam132b*), allowing for iron export via FPN.[1] The intestinal iron absorption machinery is also controlled locally by mechanisms acting within duodenal enterocytes. This includes the regulation of *Dmt1* and *Fpn* transcription and possibly ferritin turnover by hypoxia inducible factor 2 (HIF2).[6–8]

Four *Dmt1* mRNA isoforms with distinct 5′ and 3′ ends are transcribed from the *Dmt1* locus.[3] 3′ variants harbor or lack an iron-responsive element (IRE) in their 3′ untranslated region (UTR). IREs are cis-regulatory hairpin RNA structures that bind iron regulatory proteins (IRP)-1 and -2 in iron-deficient cells to modulate RNA decay or translation, respectively.[1] IRE-containing *Dmt1* mRNA variants predominate in the intestine, suggesting possible involvement of the IRP/IRE system in local regulation of DMT1.[3] Recently, we generated a mouse line with targeted disruption of the *Dmt1* 3′IRE (*Dmt1*$^{IRE\Delta}$).[9] Our work revealed that the *Dmt1* IRE exerts age-dependent effects on intestinal DMT1 expression and body iron homeostasis under standard laboratory conditions.[9] Here, we set out to determine the role of the *Dmt1* 3′IRE in the regulation of the intestinal iron absorption machinery in response to stimuli that heighten the iron demand in adults.

We first studied the role of the *Dmt1* 3′IRE in the response to chronic dietary iron restriction. *Dmt1*$^{IRE+/+}$ (or wild-type, WT) and *Dmt1*$^{IRE\Delta/\Delta}$ mice were maintained on an iron-deficient (<10 ppm Fe) versus control (~200 ppm Fe) diet from postweaning until 12 weeks of age (Figure 1A). Both WT and *Dmt1*$^{IRE\Delta/\Delta}$ animals exhibit a marked reduction of serum iron concentration when fed with low iron, associated with an increase in transferrin (Tf) levels and a decrease in Tf saturation (Figure 1B). Organismal iron stores are depleted, as evidenced by a reduction of serum ferritin, at least in KO mice (Figure 1B), and a diminution of the hepatic iron content (Figure 1C). As expected, the low iron regimen and the ensuing systemic iron deficiency lower hemoglobin levels in both genotypes (Suppl. Table S1). This is associated with elevation of circulating erythropoietin (EPO) levels (Figure 1D, left), reticulocyte frequency (Figure 1D, right), and serum ERFE concentration (Figure 1E). The reticulocytosis together with the reduction of body iron levels results in a stark drop in hepcidin (Figure 1F). Collectively, these data reflect a typical situation of iron-deficiency anemia.[10]

Histological examination of the duodenum shows enriched iron content deposited in the villi of *Dmt1*$^{IRE\Delta/\Delta}$ duodena, in comparison to WT (Figure 1G, bottom), recapitulating formerly

[1]Division of Virus-Associated Carcinogenesis (F170), German Cancer Research Center (DKFZ), Heidelberg, Germany
[2]Biosciences Faculty, University of Heidelberg, Germany
[3]Light Microscopy Facility (LMF), German Cancer Research Center (DKFZ), Heidelberg, Germany
[4]Universite de Toulouse, INSERM, CNRS, Institut Toulousain des Maladies Infectieuses et Inflammatoires (Infinity), Université Paul Sabatier (UPS), Toulouse, France

Supplemental digital content is available for this article.

HemaSphere (2022) 6:3(e693).
http://dx.doi.org/10.1097/HS9.0000000000000693.
Received: October 18, 2021 / Accepted: January 28, 2022

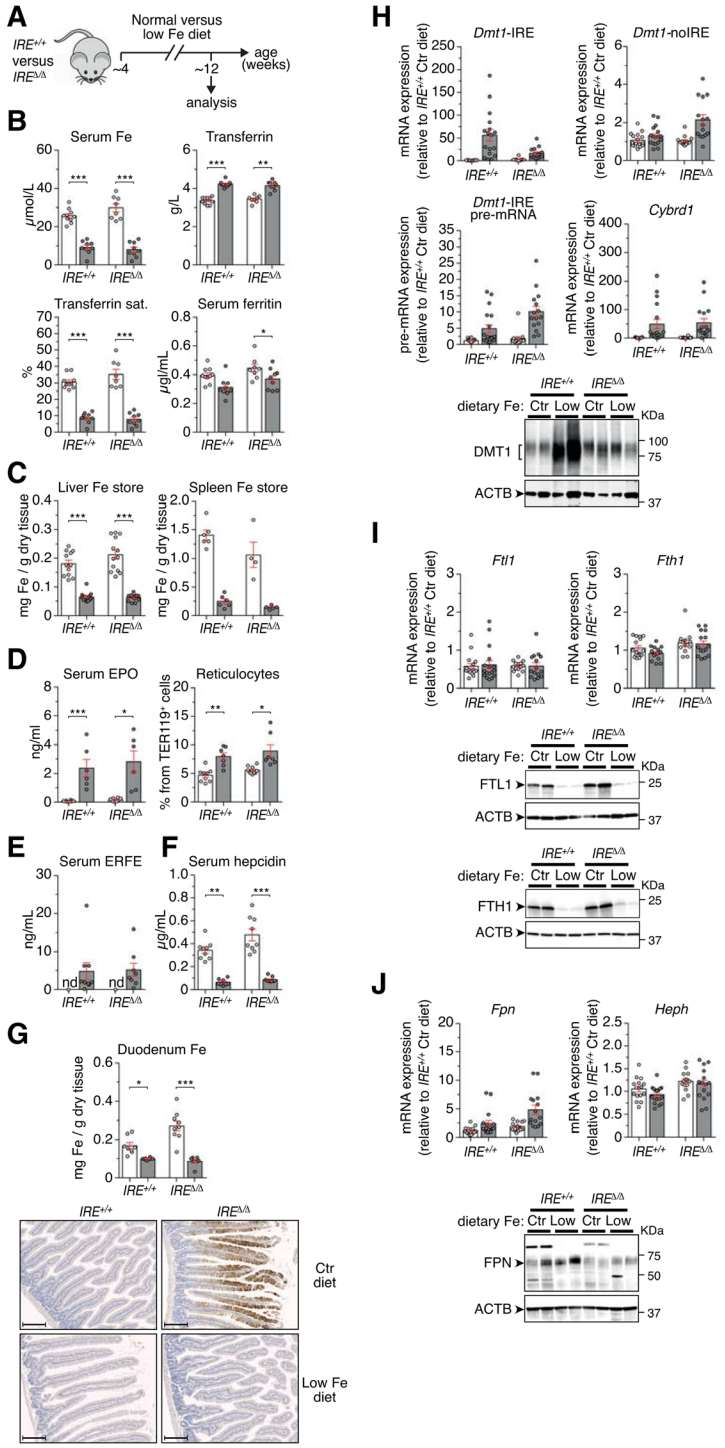

Figure 1. The Dmt1 3′IRE is required for full stimulation of duodenal DMT1 expression during chronic dietary iron defficiency. (A) WT (indicated *IRE*$^{+/+}$) and *Dmt1*$^{IRE\Delta/\Delta}$ (indicated *IRE*$^{\Delta/\Delta}$) mice, respectively, were fed with a low (<10 ppm, gray bars) versus a Ctr iron diet (~200 ppm, white bars) from weaning age on untill early adulthood (12 weeks of age); (B) serum iron parameters; (C) hepatic iron store; (D) serum EPO levels and percentage of reticulocytes among TER119^{+} blood cells. (E, F) Circulating levels of ERFE and hepcidin; the stress hormone ERFE (E) could not be detected under basal conditions (indicated nd). (G) Top histogram: iron content per mg of dry duodenal tissue. Bottom panels: Perl's staining (ehanced with diaminobenzidine) in the duodenum revealing iron deposits in intestinal epithelial cells of *Dmt1*$^{IRE\Delta/\Delta}$ fed with the Ctr diet; iron remains below the detection limit in mice receiving the low iron regimen, regardless of genotype (counterstain: hämalaun; scale bar: 200 µm). (H) Top histograms: qRT-PCR analysis of iron uptake molecules in the duodenum. Bottom panels: representative western-blot analysis of DMT1 protein expression in the duodenum, showing blunted DMT1 stimulation in *Dmt1*$^{IRE\Delta/\Delta}$ versus *Dmt1*$^{IRE+/+}$ mice. DMT1 runs as a smear, the asterisk indicates a cross-reactive band. (I) Duodenal expression of the *Fth1* and *Ftl1* iron storage molecules was assessed by qRT-PCR (top histograms) and western blotting (lower panels), respectivley. The representative western blot shows a marked decrease in ferritin protein levels in iron deficient duodena. (J) Top: qRT-PCR analysis of *Fpn* (left) and *Heph* (right) expression in the duodenum. bottom panels: western blot analysis FPN protein levels. In H to J, qRT-PCR results are presented as fold change over WT mice fed with the Ctr diet. Average mRNA levels of *Actb*, *Tubb5*, and *Gapdh* served as reference except in G, where *Dmt1*-IRE pre-mRNA levels were calibrated to *Actb* pre-mRNA expression. In H to J, ACTB served as loading control for western blotting. Statistical significance was determined using 2-way ANOVA with Tuckey's multiple comparisons test, and a *P* value inferior to 0.05 was considered significant. In B to C, n = 8 to 15. In D to G, n = 6 to 10. In H to J, n = 14 to 17. **P* < 0.05, ***P* < 0.01, ****P* < 0.001, *****P* < 0.0001. ACTB = beta actin; Ctr = control; Cybrd1 = cytochrome b reductase 1; DMT1 = Divalent metal transporter 1; EPO = erythropoietin; ERFE = erythroferrone; FPN = ferroportin; FTH1 = ferritin heavy chain 1; FTL1 = ferritin light chain 1; GAPDH = glyceraldehyde-3-phosphate dehydrogenase; HEPH = hephaestin; IRE = iron-responsive element; qRT-PCR = real-time quantitative reverse transcription PCR; sat. = saturation; TUBB5 = tubulin, beta 5 class I; WT = wild-type.

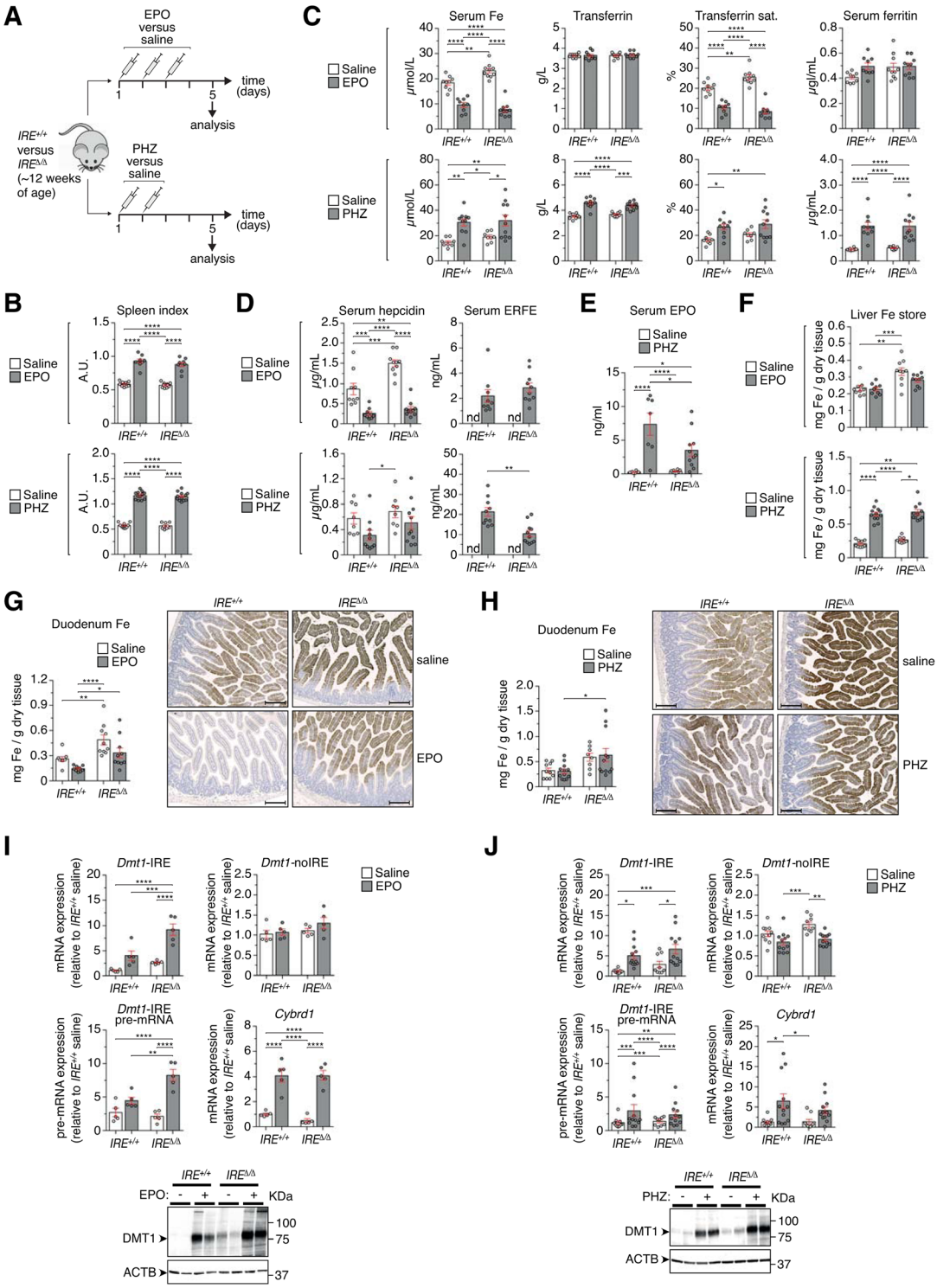

Figure 2. The Dmt1 3′IRE is dispensable for duodenal induction of DMT1 in conditions of stress erythropoiesis. (A) Adult WT (*IRE*$^{+/+}$) and *Dmt1*$^{IRE\Delta/\Delta}$ (*IRE*$^{\Delta/\Delta}$) mice were subjected to acute stress erythropoiesis. The animals were either treated with EPO (top) or with PHZ (bottom), as indicated. (B) Spleen index (calculated as square root of 100× spleen weight/body weight). (C) Serum iron parameters. (D) Serum levels of ERFE and hepcidin; ERFE was not detected in saline-injected mice (indicated nd). (E) Serum EPO concentration in mice treated with PHZ. (F) Hepatic iron store. (G, H) Duodenal iron metabolism: the bar graphs on the left display the iron content per mg of dry tissue in EPO (G) versus PHZ (H)-injected animals; the histology pictures show iron staining of duodenal villi (Perl's staining enhanced with diaminobenzidine; counterstain: hämalaun; scale bar: 200 µm). (I, J) top histograms: qRT-PCR analysis of *Dmt1* and *Cybrd1* transcripts in the duodenum of animals treated with EPO (I) or with PHZ (J), respectively. Bottom panels: representative western-blot analysis of DMT1 protein expression in the duodenum of EPO (I) versus PHZ (J)-injected mice. The expression of apical iron transport molecules augments in mice exposed to erythropoietic stresses regardless of genotype. In (I) and (J), qRT-PCR results are presented as fold change over WT mice injected with saline. Average mRNA levels of *Actb*, *Tubb5* and *Gapdh* served as reference except for the analysis of *Dmt1*-IRE pre-mRNA levels, which were calibrated to *Actb* pre-mRNA expression. For western blotting, ACTB served as loading control. Statistical significance was determined using 2-way ANOVA with Tuckey's multiple comparisons test, and a *P* value inferior to 0.05 was considered significant. In (B) to (G), n = 9 to 10 (EPO) or n = 8 to 12 (PHZ). In (I) and (J); n = 5 (EPO) or n = 9 to 12 (PHZ). **P* < 0.05, ***P* < 0.01, ****P* < 0.001, *****P* < 0.0001. ACTB = beta actin; Cybrd1 = cytochrome b reductase 1; DMT1 = Divalent metal transporter 1; EPO = erythropoietin; ERFE = erythroferrone; IRE = iron-responsive element; PHZ, phenylhydrazine; qRT-PCR = real-time quantitative reverse transcription PCR; sat. = saturation; WT = wild-type.

reported observations.[9] The low iron regimen, however, strongly depletes the duodenal iron content in both WT and mutant mice (Figure 1G, top).

At the molecular level, chronic iron deficiency triggers a substantial and selective increase in the expression of the *Dmt1*-IRE mRNA isoform in WT animals (Figure 1H, top left histogram), which translates as increased DMT1 protein levels (Figure 1H, bottom panels). This response is accompanied by an upregulation of the immature *Dmt1*-IRE pre-mRNA (Figure 1H, bottom left histogram). Most likely, iron depletion in duodenal enterocytes activates HIF2, which in turn stimulates *Dmt1*-IRE transcription.[7,8] This notion is further supported by the concomitant upregulation of another HIF2-target, *Cybrd1* (Figure 1H, bottom right histogram).[7] Similar to WT, *Dmt1*$^{IRE\Delta/\Delta}$ mice subjected to chronic iron scarcity display higher expression of both the immature *Dmt1*-IRE pre-mRNA and the *Cybrd1* mRNA (Figure 1H, bottom histograms), consistent with increased HIF2 activity. The augmentation of *Dmt1*-IRE pre-mRNA levels is even twice as high as in WT iron-deficient duodena. However, the expression of the mature *Dmt1*-IRE mRNA is only mildly augmented and is lower than in WT (Figure 1H, upper left histogram), and DMT1 protein induction is blunted (Figure 1H, bottom panels), indicating that disruption of the *Dmt1* 3′IRE impairs *Dmt1* posttranscriptional stimulation under conditions of chronic dietary iron deficiency. Despite the blunted DMT1 response, systemic iron metabolism parameters remain globally within normal range, potentially due to compensatory effects. In addition to stimulation of apical iron transport molecules, the low iron regimen and subsequent reduction of mucosal iron levels lead to diminished expression of the FTH1 and FTL1 iron storage proteins without concomitant change in the level of the corresponding mRNAs, both in WT and *Dmt1*$^{IRE\Delta/\Delta}$ duodena (Figure 1I), possibly reflecting ferritin degradation[6] or suppression of ferritin translation by the IRPs.[11] Chronic iron deficiency also augments the expression of FPN at the protein level, and the response in WT mice slightly exceeds that of mutant animals (Figure 1J, lower panels). The low iron diet has globally little or no impact on *Fpn and Heph* mRNA levels (Figure 1J, histograms). Collectively, these results indicate that stimulation of *Dmt1*-IRE transcription by HIF2 does not suffice, and that posttranscriptional stimulation of *Dmt1* through the 3′IRE is additionally required for full stimulation of intestinal DMT1 expression in response to chronic dietary iron deficiency.

We next assessed the role of the *Dmt1* 3'IRE in the response to stress erythropoiesis, a condition that acutely increases the erythroid iron demand and thus stimulates the intestinal iron absorption machinery. Mice were injected either with recombinant EPO to stimulate erythropoiesis directly,[11] or phenylhydrazine (PHZ) to mimic acute hemolytic anemia, a situation that also enhances erythropoiesis (Figure 2A).[12] As expected, both treatments trigger extramedullary erythropoiesis, as indicated by a marked increase in spleen size in all genotypes (Figure 2B). Accordingly, EPO treatment augments hemoglobin levels (Suppl. Table S1) as well as reticulocyte frequency in peripheral blood, as measured by flow cytometry (WT: 14.3% ± 1.0% versus 5.8% ± 1.2% reticulocytes among TER119^{+} cells in EPO-treated versus control mice; *Dmt1*$^{IRE\Delta/\Delta}$, 14.1 ± 1.1 and 4.6% ± 0.5%, respectively); reticulocytosis could not be assessed reliably in PHZ-treated mice due to autofluorescence from damaged RBCs (not shown). Expansion of the erythroid compartment in EPO-treated mice increases iron consumption and thus lowers serum iron and transferrin saturation values (Figure 2C), while inducing ERFE and suppressing serum hepcidin (Figure 2D). EPO does not affect hepatic iron levels (Figure 2F), but the amount of iron in duodenal villi tends to be reduced (Figure 2G). Differing from the EPO regiment, the release of iron from damaged RBCs in PHZ-treated mice results in an elevation of systemic iron indices in both WT and *Dmt1*$^{IRE\Delta/\Delta}$ animals, with high serum iron and ferritin concentration, high transferrin saturation values, and iron accumulation in the liver (Figure 2C,F). Yet, the marked reduction of RBC counts (Suppl. Table S1) enhances EPO and ERFE production (Figure 2D,E), albeit to a lesser extent in *Dmt1*$^{IRE\Delta/\Delta}$ mice. Despite high ERFE levels, the reduction in hepcidin does not reach statistical significance (Figure 2D). While EPO treatment tends to decrease the duodenal iron content (Figure 2G), this is not the case in PHZ-treated animals (Figure 2H). Consistent with an elevation of iron needs, treatment with either EPO or PHZ significantly increase the levels of the *Cybrd1* mRNA and the immature *Dmt1*-IRE pre-mRNA in *Dmt1*$^{IRE\Delta/\Delta}$ duodena (Figure 2I). However and in sharp contrast to chronic dietary iron deficiency (Figure 1H), the absence of a functional *Dmt1* 3′IRE in *Dmt1*$^{IRE\Delta/\Delta}$ mice does not weaken the induction of the mature *Dmt1*-IRE mRNA nor the stimulation of DMT1 protein expression under conditions of stress erythropoiesis (Figure 1I,J). Mirroring duodenal iron levels, ferritin protein expression is decreased in EPO, but barely affected in PHZ-treated mice, regardless of genotype (Suppl. Figure S1A,B). FPN protein expression is augmented in all genotypes (Suppl. Figure S1C,D). mRNA levels of *Fth1*, *Ftl1*, and *Heph* are barely affected, *Fpn* mRNA expression is mildly induced by EPO (Suppl. Figure S1A–D). Overall, these data show that the *Dmt1* 3′IRE is largely dispensable for adequate regulation of key intestinal iron absorption molecules in conditions of acute erythropoietic stress.

We have formerly reported a strong posttranscriptional downregulation of *Dmt1*-IRE mRNA expression in *Dmt1*$^{IRE\Delta/\Delta}$ duodena during the suckling period,[9] a stage of life characterized by high iron needs, low iron stores, and relatively limited iron supply from maternal milk.[13,14] This phenomenon, however, was not recapitulated in adult mice under steady-state conditions, uncovering an age-dependent switch in the activity of the *Dmt1* 3'IRE in the intestine. With the inability to replenish supply from dietary source, WT mice fed with an iron-poor diet over a long period of time respond by enhancing duodenal *Dmt1-IRE* expression. By contrast and despite a marked stimulation of *Dmt1*-IRE transcription, adult *Dmt1*$^{IRE\Delta/\Delta}$ mice exhibit low levels of *Dmt1-IRE* both at the mature mRNA and protein level. Hence, a functional IRE loop in the 3′UTR of the *Dmt1* mRNA appears to be needed to properly adjust DMT1 expression during long-term iron scarcity, as observed in suckling mice[9] and in animals subjected to dietary iron deficiency (this study). Conceivably, and by analogy to other 3'IRE motifs, IRP binding to the *Dmt1*-3′IRE stabilizes the transcript, which together with stimulation of *Dmt1* transcription by HIF2 is needed to achieve adequate DMT1 protein expression. In contrast to dietary iron restriction, both EPO and PHZ treatments represent acute increases in systemic iron demands in mice already loaded with iron. Our results indicate that the loss of IRE function in *Dmt1* does not affect the overall response to acute erythropoietic stress. This implies that the observed upregulation of duodenal DMT1 expression is largely IRE/IRP-independent and is likely mediated by HIF2.[15] Among other possibilities, the degree of iron depletion in absorptive enterocytes (more profound in chronic dietary iron deficiency than upon EPO or PHZ treatements) might influence the contribution of IRP/IRE binding and HIF2, to the regulation of DMT1.

In addition to the age- or tissue-dependent effects on DMT1 expression reported previously,[9] the *Dmt1* 3′IRE now appears to also influence DMT1 regulation in a stimulus-dependent manner. Whether the context-dependent activity of the *Dmt1* 3′IRE involves the luminal or enterocytic iron status, the gut microbiome, and additional molecules whose activity is also situation-dependent warrants further research.

ACKNOWLEDGMENTS

We are grateful to H. Gunshin and N.C. Andrews for sharing the *Dmt1*$^{IRE\Delta}$ mouse line. We thank the staff of the "Center for Preclinical Research" of the DKFZ for their dedicated care of the animals, and the "Plateforme de Biochimie" at the "Centre de Recherche sur l'Inflammation" (Paris, France) for their measurement of serum parameters.

AUTHOR CONTRIBUTIONS

MQ and BG designed the research. MQ, MB, GP, AE, GS, MP-S, and BG performed experiments. MQ, MB, ZK, and BG analyzed the data. MQ, ZK, and BG wrote and reviewed the article.

DISCLOSURES

The authors have no conflicts of interest to disclose.

SOURCES OF FUNDING

This work was supported by a grant from the Deutsche Forschungsgemeinschaft to BG (GA2075/5-1).

REFERENCES

1. Muckenthaler MU, Rivella S, Hentze MW, et al. A red carpet for iron metabolism. *Cell*. 2017;168:344–361.
2. Ganz T. Systemic iron homeostasis. *Physiol Rev*. 2013;93:1721–1741.
3. Shawki A, Knight PB, Maliken BD, et al. H(+)-coupled divalent metal-ion transporter-1: functional properties, physiological roles and therapeutics. *Curr Top Membr*. 2012;70:169–214.
4. Anderson GJ, Frazer DM. Current understanding of iron homeostasis. *Am J Clin Nutr*. 2017;106(suppl 6):1559S–1566S.
5. Nemeth E, Ganz T. Hepcidin-ferroportin interaction controls systemic iron homeostasis. *Int J Mol Sci*. 2021;22:6493.
6. Das NK, Sankar A, Schwartz AJ, et al. Intestinal ferritinophagy is regulated by HIF-2α and is essential for systemic iron homeostasis. *BioRxiv*. 2020;11.01.364059. https://doi.org/10.1101/2020.11.01.364059.
7. Shah YM, Matsubara T, Ito S, et al. Intestinal hypoxia-inducible transcription factors are essential for iron absorption following iron deficiency. *Cell Metab*. 2009;9:152–164.
8. Mastrogiannaki M, Matak P, Keith B, et al. HIF-2alpha, but not HIF-1alpha, promotes iron absorption in mice. *J Clin Invest*. 2009;119:1159–1166.
9. Tybl E, Gunshin H, Gupta S, et al. Control of systemic Iron homeostasis by the 3' iron-responsive element of divalent metal transporter 1 in mice. *HemaSphere*. 2020;4:e459.
10. Koleini N, Shapiro JS, Geier J, et al. Ironing out mechanisms of iron homeostasis and disorders of iron deficiency. *J Clin Invest*. 2021;131:148671.
11. Galy B, Ferring-Appel D, Becker C, et al. Iron regulatory proteins control a mucosal block to intestinal iron absorption. *Cell Rep*. 2013;3:844–857.
12. Latunde-Dada GO, Vulpe CD, Anderson GJ, et al. Tissue-specific changes in iron metabolism genes in mice following phenylhydrazine-induced haemolysis. *Biochim Biophys Acta*. 2004;1690:169–176.
13. Frazer DM, Darshan D, Anderson GJ. Intestinal iron absorption during suckling in mammals. *Biometals*. 2011;24:567–574.
14. Lönnerdal B. Development of iron homeostasis in infants and young children. *Am J Clin Nutr*. 2017;106:1575S–1580S.
15. Schwartz AJ, Das NK, Ramakrishnan SK, et al. Hepatic hepcidin/intestinal HIF-2α axis maintains iron absorption during iron deficiency and overload. *J Clin Invest*. 2019;129:336–348.